Bull. Chem. Soc. Ethiop. **2024**, 38(6), 1609-1624.
DOI: https://dx.doi.org/10.4314/bcse.v38i6.9

ISSN 1011-3924
Printed in Ethiopia
Online ISSN 1726-801X

DESIGN, CHARACTERIZATIONS, DFT, MOLECULAR DOCKING AND ANTIBACTERIAL STUDIES OF SOME COMPLEXES DERIVED FROM 4-AMINPANTIPYRINE WITH GLYCINE AMINO ACID LIGAND

Baraa Abdul-Khaleq Mohammed*, Sahbaa Ali Ahmed* and Fanar Al-Healy

University of Mosul, College of Science, Department of Chemistry, Ninevah, Iraq

(Received March 26, 2024; Revised June 9, 2024; Accepted June 12, 2024)

ABSTRACT. The synthesis of the heterocyclic ligand (LK) involved the combination of 4-amino antipyrine, 4-nitroacetophenone, and glycine. A new series of transition metal complexes of Ni(II), Co(II), Cu(II), and Zn(II) have been synthesized from the Schiff base (LK). It was characterized by micro elemental analysis, FT-IR, UV-Vis, and ^{1}H-NMR spectroscopy. The prepared complexes were characterized using (CHN) analysis, flame atomic absorption, as well as conductivity measurements and magnetic susceptibility. From the obtained data, the octahedral structure was suggested for all complexes. The ligand showed tridentate nature by binding to metal ions through the N atom of antipyrine and the N,O atom of glycine. The exhibited excellent electrolytic properties, except for the Cu(II) and Zn(II) complex which exhibited non-electrolytic behavior. Theoretical calculations with DFT were conducted for all complexes. The antibacterial activity of the ligand and its complexes against (*S. aureus*, *B. subtilis*) was evaluated through the disc diffusion method. Additionally, molecular docking analysis was conducted to gain more insights into the ligand's binding energy and interaction with the *S. aureus* receptor.

KEY WORDS: 4-Amino antipyrine, Heterocyclic ligand, Glycine, Molecular docking

INTRODUCTION

Schiff base ligands are derived from the condensation reaction of ketones or aldehydes with primary amines [1]. Schiff bases are an essential class of organic molecules that have many applications in many fields, such as biological, analytical, and inorganic chemistry [2]. Some of these molecules act as catalysts in polymers and dyes. Furthermore, Schiff bases have become significant in the fields of pharmacology and medicine because of their diverse range of biological properties: like antiviral, anti-inflammatory, antimicrobial, antifungal [3], analgesic anticonvulsant, antioxidant, anthelmintic, antimalarial [4], antitubercular, and anticancer [5]. Antipyrine an N-heterocyclic compound and its derivatives exhibit a wide range of biological activities. 4-Amino group is considered therapeutic groups most commonly detected in water are: analgesics, antidepressants, antiepileptics, lipid-lowering drugs, and antihistamines, Figure 1 [6]. The coordination chemistry of 4-aminoantipyrine complexes involving oxygen and nitrogen donor ligands, has excited great interest among chemists in recent years due to their applications in catalysis which are related to the ecosystem and human health. Copper(II) and zinc(II) are life essential metallic elements with biochemical activity when interactions with specific proteins, participating in oxygen transport, the storage of ions and electronic transfer reactions [5]. In this study, we present the facile synthesis and spectral studies of a Schiff base, potassium 2-((1,5-dimethyl-4-(((E)-1-(4-nitrophenyl) ethylidene) amino)-2-phenyl-1,2-dihydro-3H-pyrazol-3-ylidene) amino) acetate (LK). Four transition metal complexes were synthesized from the ligand (LK), and characterized by using multiple analytical techniques. The ligand and its complexes were tested for their antibacterial activity against *S. aureus* and *B. subtilis*. Additionally, density functional theory (DFT) calculations were performed for the synthesized ligand. Furthermore, simulations of molecular docking were also carried out to try to learn more about the potent antibacterial activity of the produced ligand and the *S. aureus* receptor's binding sites.

*Corresponding authors. E-mail: baraa.23scp51@student.uomosul.edu.iq, sahbaa-ali@uomosul.edu.iq

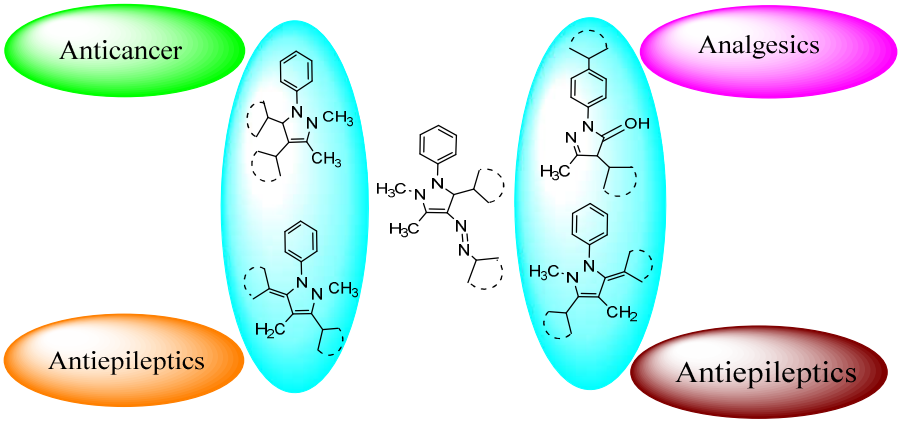

Figure 1. Some of medical applications for the antipyrine nucleus.

EXPERIMENTAL

Chemicals and solvents

Chemicals were purchased from Sigma-Aldrich and Merck and used without further purification. Co(II) chloride, Zn(II) chloride, Cu(II) chloride, Ni(II) chloride, and 4-aminoantipyrine, glycine amino acid. Organic solvents such as ethanol, methanol, acetone petroleumether, dimethyl sulfoxide (DMSO) and dimethylformamide (DMF) were spectroscopically pure obtained from BDH.

Synthesis

Synthesis of the Schiff-bases ligand (LK) [6-9].

Step 1. A solution of (2. 03g, 0.01 mol) 4-aminoantipyrine (**1**) in 15 mL of ethanol was added to a solution of (1.65 g, 0.01 mol) 4-nitroacetophenone (**2**) in 15 mL of ethanol and 0.2 mL of glacial acetic acid, was heated on a water bath for 3 hours with reflux. The reaction was monitored using thin layer chromeatography (TLC). After cooling to room temperature, the orange crystals were filtered, washed with ethanol and recrystallized in methanol to obtain the compound (**3**), (E)-1,5-dimethyl-4-((1-(4-nitrophenyl)ethylidene)amino)-2-phenyl-1,2-dihydro-3H-pyrazol-3-one; orange crystals, yield: 77%, m.p.: 148 °C, is shown in Scheme 1.

Step 2. In a round-bottom flask, (0.3 g, 0.04 mol) of glycine amino acid was dissolved in (20 mL) of a 1:1 H_2O-ethanol solution. Then (20 mL) of a hot ethanolic solution of KOH (0.22 g) was added; the mixture stirred to create a uniform solution. Refluxing for three hours followed the addition of the compound (**3**). The same ratio was added to the previous mixtures and refluxed for 3 hours. The reaction was monitored by TLC. A dark orange crystal precipitate was formed and filtered off, washed several times with ethanol, then recrystallized in methanol and dried to give the (LK) ligand, is shown in Scheme 1.

Synthesis of the metal complexes

The Schiff base ligand (LK) (0.445 g, 0.001 mol) was dissolved in ethanol. The following ethanolic metal salt solutions were added to the (LK) ligand, solution at the molar ratio (1L:1M): 0.2379 g Co(II), 0.2377 g Ni(II), 0.1704 g Cu(II), and 0.2444 g Zn(II). The mixture was refluxed and stirred for 4 h at 85 °C. The resultant product was filtered and repeatedly cleaned with a water-MeOH solution (1:2), and petroleum ether [5, 9]. The synthesized complexes were dried in a vacuum desiccator, and finally recrystallized from methanol. The route of synthesis is shown in Scheme 1.

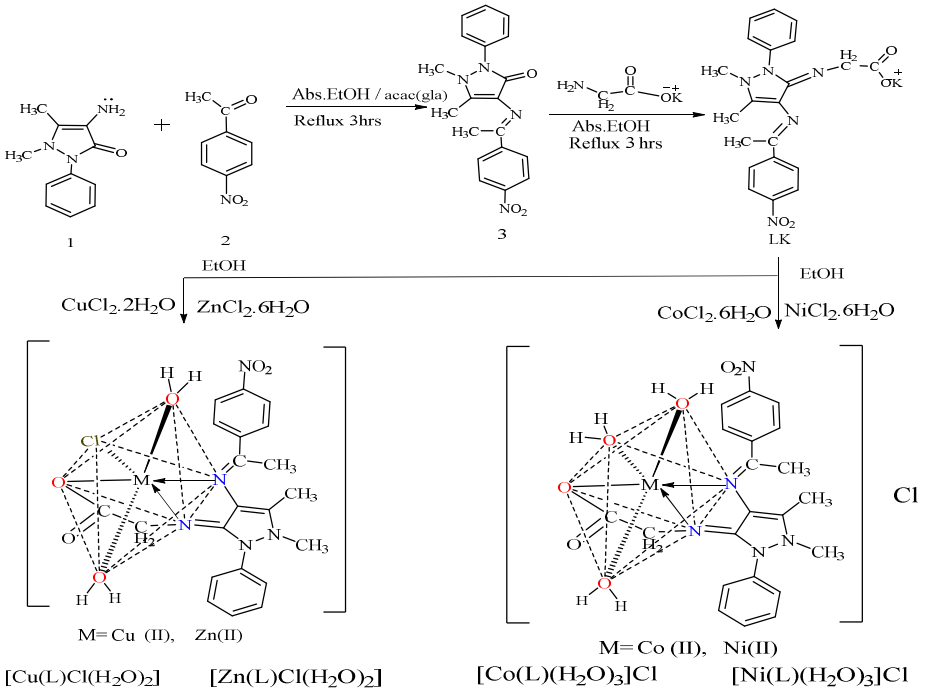

Scheme 1. Preparation of the ligand (LK) and corresponding metal complexes.

Characterization

The open capillary method was used for the detection of melting points and was uncorrected by Stuart-SMP10. The spectral analyses were carried out at the Department of Chemistry, Gaziosmanpaşa Üniversitesi, Tokat, Turkey. Elemental microanalysis recorder by using the Elementar Vario Micro Cube. ^{1}H NMR spectra were determined on (Bruker Bio Spin GmbH, 400 MHz), tetramethyl silane was used as an internal reference, and chemical shifts are quoted in δ (ppm). X,pert Philips Holland was utilized to obtain XRD patterns, the FT-IR spectrum was recorded reflectively on a spectrophotometer (ATR, Alpha platinum, Bruker) in wave number (400–4000 cm^1), and electrical conductivity measurements of the complexes were recorded at 25 ºC using a conductivity meter (model 4510–Jenway), measured the samples' (10^{-3} mol L^{-1}) solutions of the synthesized compounds in DMF were determined using Magnetic Susceptibility Balance Mode (MSB_MKI). The electronic spectra were recorded in DMF (UV-Vis)

spectrophotometer type UV analytikjenaometer, atomic absorption spectrometry (ICP-AES). The stoichiometry of the compounds was determined using a continuous-variation spectrophotometric method. The reactions were monitored by (TLC) using silica gel 60 F_{254} (Merck, Darmstadt) and compounds were visualized by exposure to UV.

Powder XRD

X-ray powder data were especially helpful in determining precise cell characteristics when a single crystal was not available. The complex's crystalline structure is confirmed by the diffraction pattern. The Cu(II) and Zn(II) complexes' XRD patterns, which ranged from10 -75º (θ) at a wavelength of 1.54 Å, are shown in Figure 3a,b.

DFT modeling

Sometimes there is no crystal structure. In order to understand further about the molecular structures of the (LK) ligand and its complexes, computer investigations were performed. The software 09 W Gaussian was used for geometric optimizations. The complexes singlet ground state molecular geometries in the gas phase were thoroughly optimized at the B3LYP level of theory, in Figure 2. While LANL2DZ [10, 11] was used to model the Co(II), Ni(II), Cu(II), and Zn(II) atoms and ligand atoms were modeled using the 6–311 (d,p) basis set. The compounds during investigation were found to have optimal geometries, and their molecular border orbitals, LUMO (lowest unoccupied molecular orbital) and HOMO (highest occupied molecular orbital), were also identified. Using the HOMO and LUMO energies, the values of chemical hardness (η), softness (σ), electronegativity (χ), energy gap (ΔE) nucleophilicity (η), and electrophilicity index (ω)were calculated [9, 10]. The results of the calculation are shown in Table 2.

Molecular docking studies

A widely used method to identify structure-based activity interactions is molecular docking. It additionally makes the ability to predict and confirm a small-molecule ligand's binding to specific target protein binding sites. The Auto Dock Vina1.1.2 program was used in this study to study docking. Crystal structure retrieval: We utilized the RCSB Protein Data Bank to obtain the active site crystal structure of the *S. aureus* receptor in order to carry out the docking calculations. For this specific structure, the PDB ID is 2H92 and ID:2CCJ. The ChemAxon Marvin Sketch 5.3.735 program was used to create and conform the ligand's three-dimensional structure, which was then saved in the mol2 format. The optimization and energy minimization of the ligand structure were conducted by the Gaussian 09 software. Prior to the docking calculations, all water molecules and the ligand were removed [12,13], analysis of ligand-protein interaction to analyze the interaction between the ligand and the targeted protein. The results of molecular docking were visualized in (BIOVIA, Discovery Studio, v4.0.100.13345).

Antibacterial activity

The agar-disc diffusion method was used to evaluate the antibacterial effects of three different substances. In this technique, newly synthesized (LK) ligand and its complexes (25 µg/mL and 50 µg/mL of DMSO) were impregnated into a sterile disc measuring 5 mm in diameter made of filter paper (Whatman No. 1), which was then incubated for 12 hours at 37 ºC on a nutrient agar plate. After 12 hours, measurements were made of the inhibition zones surrounding the dried impregnated discs. Each disk was labeled with its unique ID number on the back of the Petri dish [13, 14]. In the same experimental conditions, the antibacterial effectiveness of the compounds under investigation. Were evaluated in comparison to the conventional antibiotic ciprofloxcin 30

µg/mL of DMSO was used as a reference drug for comparison. Table 3, showed of the zone inhibition for LK and its complexes against *Staphylococcus aureus* and *Bacillus subtilis.*

RESULTS AND DISCUSSION

Structure configuration of the ligand

The prepared ligand was characterized using elemental analysis, FT-IR, and ^{1}H-NMR spectra. In the IR spectra of the ligand, the –NH_2 group and carboxylic group disappeared for the amino acid, and new bands related to the imine -C=N- group emerged at around 1682 cm^{-1} The ^{1}H-NMR spectrum in DMSO-d_6 showed signals for –N-CH_2-COO- group at δ 2.32 ppm^{-1}, aromatic proton signals from δ 8.3 to 7.35, methyl for antipyrine ring at 2.40 ppm, and methyl group for ketone-imine at 2.11 ppm.

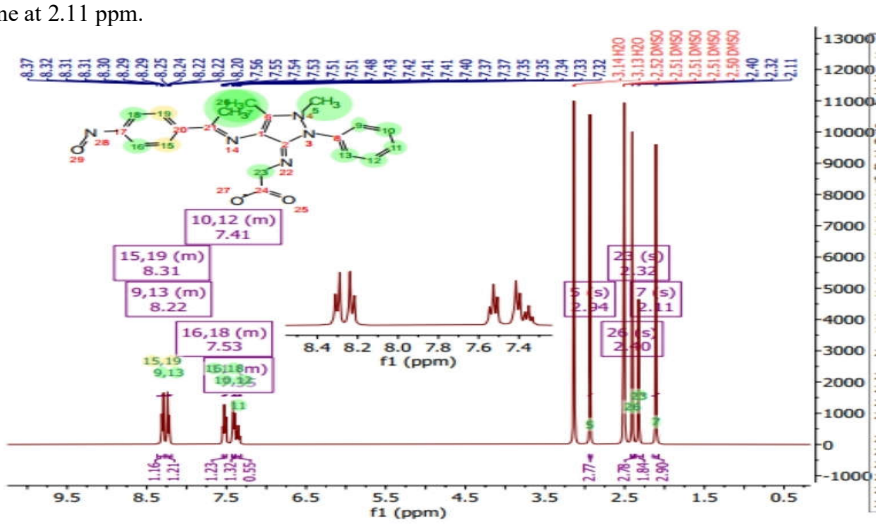

Figure 2. ^{1}H-NMR, spectrum of the free LK-ligand.

Structural characterization of the metal-ligand complexes

The solubility of the complexes in DMF and DMSO at room temperature is almost complete, but insoluble in water. Table 1 displays the analytical data and physicochemical properties of each molecule. Various techniques, such as, infrared IR, ^{1}H NMR spectroscopy, elemental analysis molar conductivity, thermal analysis and magnetic susceptibility, were utilized to analyze the structure of the (LK) ligand and its complexes. The results were a combined effort of all these methods. Spectroscopic and analytical information helped propose potential structures for the newly created metal complexes (Scheme 1). Nonetheless, analytical and spectroscopic results corroborated the hypothesized frameworks. In addition, the data obtained from the (C, H, and N) matched the expected structures. Molar conductance was conducted to test freshly prepared DMF solutions of the complexes at a concentration of 1.0 x 10^{-3} M. Prepared complexes had high molar conductivity values, indicating they were electrolytes except for Zn(II) and Cu(II), as shown in Table. 1.

Binding mode and FTIR spectra

The FTIR spectrum data illustrates how ligand interact with metal ions. Comparing IR spectra of metal complexes and free ligand can help identify coordination sites for potential chelation, as shown in Table 1.

Table 1. Physical properties UV-Vis, conductivity, magnetic, and FT-IR results.

		$C_{21}H_{20}KN_5O_4$ (LK)	$[Co(L)(H_2O)_3]Cl$	$[Ni(L)(H_2O)_3]Cl$	$[Cu(L)Cl(H_2O)_2]$	$[Zn(L)Cl(H_2O)_2]$
Color		Orange	yellow	Yellowish	Brownish	Orange
m.p.		160 ºC	220 ºC	240 ºC	230 ºC	215 ºC
Yield		78%	81%	78%	83%	80%
C.H.N. Found (calc.) %	C	56.67 (56.71)	45.58 (45.46)	45.54 (45.48)	46.68 (46.58)	46.51 (46.43)
	H	4.66 (4.53)	4.86 (4.72)	4.80 (4.73)	4.56 (4.47)	4.48 (4.45)
	N	15.79 (15.72)	12.60 (12.62)	12.70 (12.63)	11.80 (11.74)	12.90 (12.89)
	M	--	10.71 (10.62)	10.69 (10.58)	12.87 (12.93)	12.14 (12.03)
μeff (B.M)		--	4.73	3.08	2.04	diamagnetic
Conductivity	Ω-$^{1}cm^{2}mol^{-1}$		88.6	80.8	35.8	23.8
IR spectra	$\nu(OH_{broad}$ of water)	--	3233	3348	3271	3431
	$\nu(COO_{asym})$	1574	1580	1576	1581	1565
	ν(-C=N)	1682	1656	1660	1656	1665
	$\nu(COO_{sym})$	1454	1432	1434	1441	1445
	ν(M-O)	--	591	541	588	531
	ν(M-N)	--	450	446	430	440
UV-Vis (nm)	Λ_{max}	272	803 683 423	889 726 406	527	366 335
Stoichiometry	M:L	--	1:1	1:1	1:1	1:1

The imine ν(-C=N) linkage is responsible for the band that the Schiff base ligand (LK) shows at (1682 cm^{-1}). This band shifts to lower frequencies in their metal complexes' spectra, from (1656-1665 cm^{-1}). The imine nitrogen takes part in chelation with the metal ion [8, 9], based on a comparison between the Schiff base's and the complexes' IR spectra. It is anticipated that the coordination of nitrogen with the metal ion will lower the imine link's electron density, shifting the ν(-C=N) group. It is possible to identify two bands at(1565-1581 cm^{-1}) and(1432-1445 cm^{-1}) as ν(asym COO-) and ν (sym COO-). These bands are involved in coordination with the specified metal ions, as evidenced by their shift to the higher and lower areas during complex formation [5-7]. Furthermore, bands found in the complexes between (531-591cm^{-1}) and (430-450 cm^{-1}), which have been missing in the free ligand are assigned to the ν(M–O) and ν(M–N) vibrations. The appearance of bands belonging to water molecules coordinated with the metal ion in both complexes in the region (3233-3431 cm^{-1}).

Magnetic measurements and electronic spectra

Two distinct bands can be seen in the electronic spectra of the Co(II) complex, one at 423 nm, 683 nm, and 803 nm. These bands can be assigned to the $^{4}T_1g(F)\rightarrow{}^{4}T_2g(P)$, $^{4}T_1g(F)\rightarrow{}^{4}A_2g(F)$ and $^{4}T_1g(F)\rightarrow 4T_2g(F)$ transition, respectively. The estimated μeff of the LCo complex at 25 °C is 4.73 B.M., which would be ascribed to d^7 high spin ($t_2g^5eg^2$) electron configuration, suggesting the LCo complex has an octahedral geometry, Table 1. In the electronic spectra of the Ni(II) complex, three bands at 406 nm, 726 nm, and 889 nm were observed. $^{3}A_2g(F)\rightarrow{}^{3}T_1g(P)$, $^{3}A_2g\ (F)\rightarrow{}^{3}T_1g(F)$,

$^3A_2g(F)\rightarrow{}^3T_2g$ (F) transitions. The calculated μeff of LNi compound is 3.08 B.M., back to d^8 ($t_2g^6eg^2$) electron configuration, suggesting an octahedral geometry, Table1. In the electronic spectra of the Cu(II) complex, one band at 527 nm was observed and assigned to the $^2Eg\rightarrow{}^2T_2g$ transition. The intended μeff of LCu compound is 2.04 B.M., back to d9 ($t_2g^6eg^3$) electron configuration, signifying an octahedral geometry, Table 1. The electronic spectra of the Zn(II) complex showed two bands at 366 nm and 335 nm, respectively. The diamagnetic character of the LZn complex would be attributed to the octahedral geometry of the LZn complex, Table 1.

Interpretation of a complex structure

The analyzed compounds contain C, H, and N in varying proportions. The experimental section displays elemental analyses, C, H, and N, and molecular formulae of the complexes. Metal chelates have a 1:1 metal-ligand ratio. Elemental composition and molar conductivity tests confirmed structures of LK ligand with Co(II), Ni(II), Cu(II), and Zn(II) ions. The LK ligand binds to cations through one nitrogen-imine group for antipyrine, oxygen-carboxylic and nitrogen-imine group for amino acid glycine, acting as a tri-dentate ligand. Ni(II) and Co(II) chelates are electrolytes, while Cu(II) and Zn(II) chelates are non-electrolytes. Molar conductivity, μeff (B.M), and UV-Vis spectra suggest an octahedral structure for investigated metal chelates,$[Cu(L)Cl(H_2O)_2]$, $[Zn(L)Cl(H_2O)_2]$, $[Co(L)(H_2O)_3]Cl$, $[Ni(L)(H_2O)_3]Cl$ complexes correspondingly, Scheme 1.

Powder X-ray diffraction

The XRD pattern of the metal complexes exhibits well-defined crystalline peaks, indicating that the samples were in a crystalline phase. $D = K\lambda/\beta Cos\theta$ is Scherer's equation, which was used to determine the grain size of the metal Schiff base complexes, where 'β' is the full width at half maximum of the prominent intensity peak, 'θ' is the diffraction angle, 'λ' is the wavelength, and 'D' is the crystal size rate (nm). The average grain size values for the complexes are(1.77-21.27) nm,(42.36-61.83) nm suggesting that they were in a crystalline regime [9, 15].

DFT calculations

Molecular modeling is becoming more vital for analyzing the structures of coordination compounds when X-ray crystal data is unavailable, offering additional structural information and energy-minimized conformation. The compounds' three-dimensional orbitals are the outcome of HOMO and LUMO calculations performed at the DFT/B3LYP level of theory. Figure 4 shows optimized molecular structures of the LK ligand and its metal complexes using the DFT method. Figure 5.Displays the HOMO and LUMO, also known as frontier molecular orbitals, which represent the highest occupied and lowest unoccupied orbitals in a molecule. The orbital energy gap (ΔE) is related to the kinetic stability and chemical reactivity of a molecule [10-12]. The energy gap between the HOMO and LUMO states is often used as an indicator of a ligand's electronic structure. These molecules have low polarization and are referred to as "hard" molecules when the HOMO-LUMO energy difference is large. Conversely, the molecules are described as "soft" when there is minimal variation in the HOMO-LUMO energy, strong polarization, and easily influenced electron distribution. The HOMO-LUMO energy gap of the ligand and its metal chelates with Co(II), Ni(II), Cu(II), and Zn(II) ions was calculated to be 3.42, 2.28, 2.011, 1.01, and 2.56 eV, respectively. When compared to the metal complexes, the ligand's HOMO-LUMO energy gap is greater. In terms of energy gaps, the compounds are arranged as follows: L > LZn > LCo > LNi > LCu.

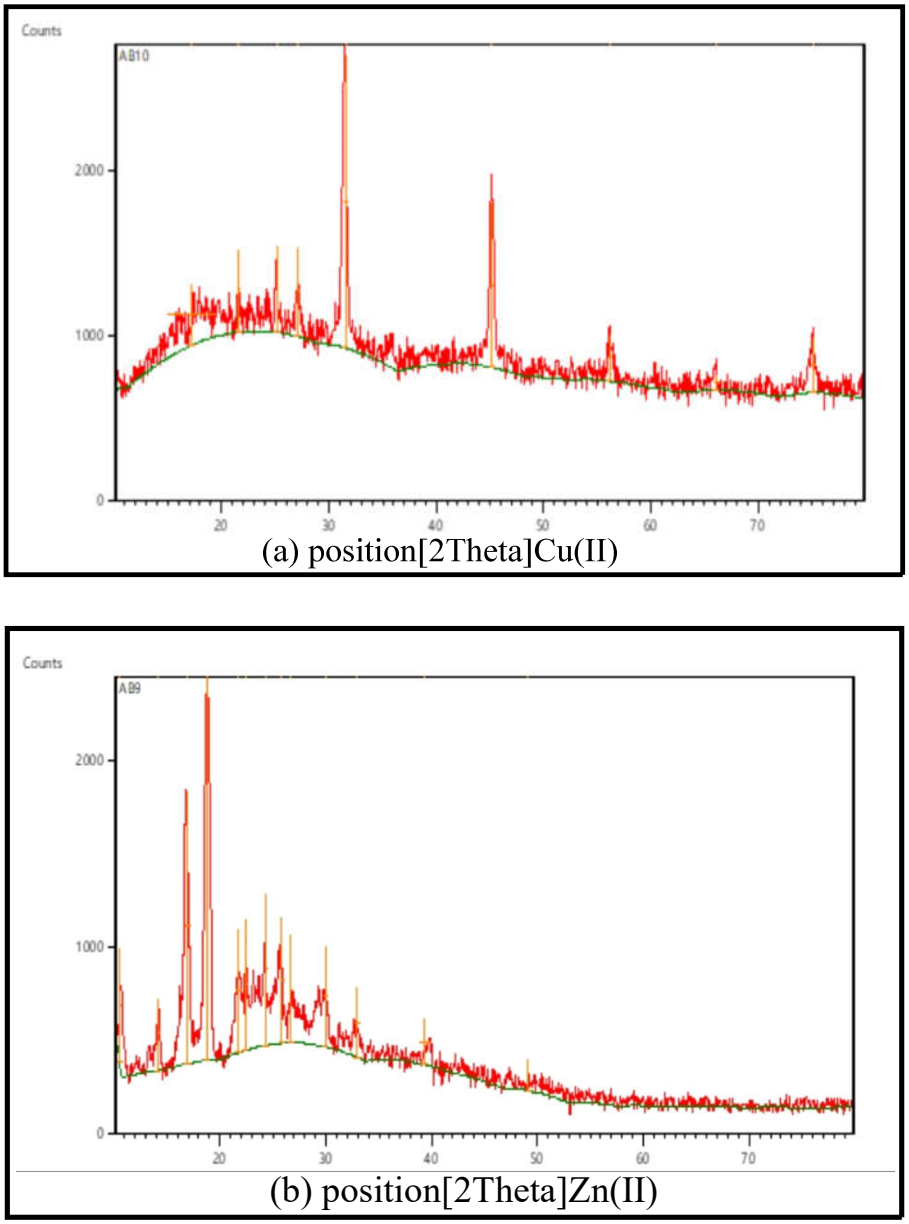

Figure 3. XRD spectra of (a) Cu(II) complex and (b) Zn(II) complex.

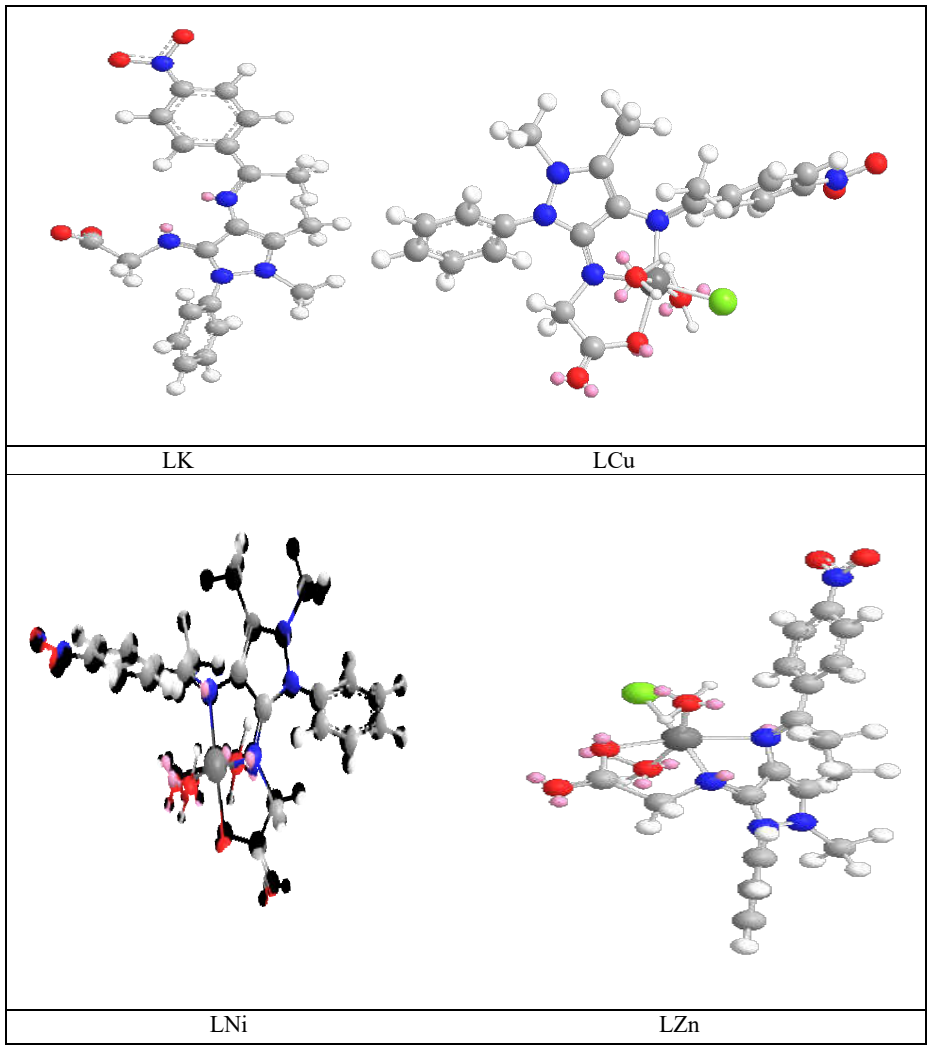

Figure 4. Optimized 3D structure of the ligand and some of its complexes.

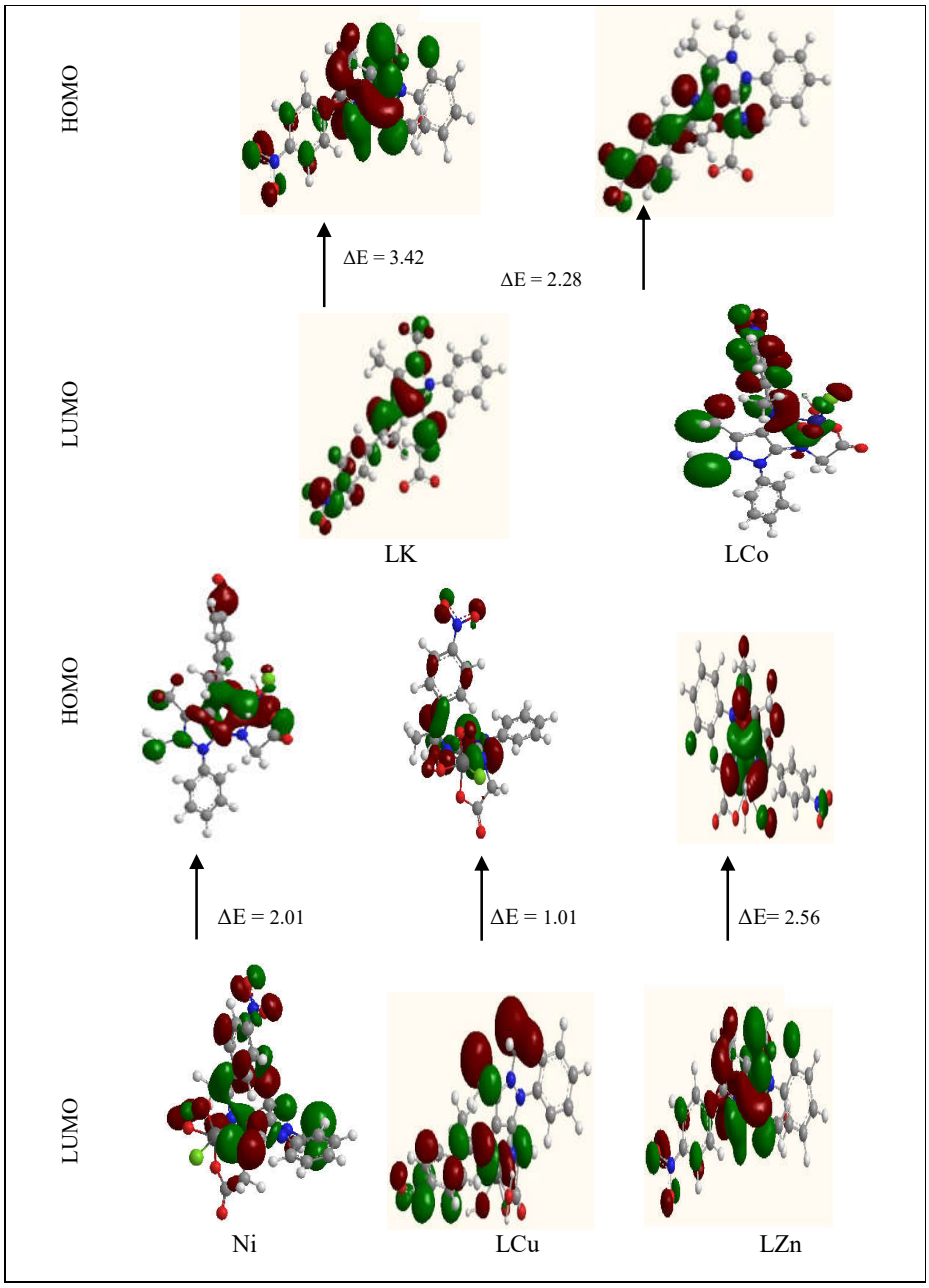

Figure 5. The HOMO and LUMO of the ligands LK and its NiL and ZnL complexes.

Determining absolute hardness (η) and softness (σ) is crucial for understanding molecular stability and reactivity. The ligand's higher binding energy signifies greater stability than the complexes. Additional parameters like CP, ω, S, χ, and ΔN_{max} were also computed for ligand and their complexes [9]. Analyzing the energy gaps between HOMO and LUMO orbitals provides vital information for assessing molecular hardness and softness. (LK) was identified as the most stable molecule, while (LCu) exhibited the highest reactivity and softness, and (LCo) was considered a neutral molecule. Chemical descriptors like η and σ are used to characterize molecular reactivity, with HOMO and LUMO energies being key in their determination. Table 2 presents the calculated results.

Table 2. The calculated quantum chemical parameters of LK and its complexes.

	EHOMO	ELUMO	ΔE	I	A	χ	CP	σ	ω
L	−5.270	−1.850	3.42	5.27	1.85	3.56	−3.560	0.29	3.710
LCo	−4.570	−2.30	2.28	4.57	2.3	3.44	−3.440	0.44	5.191
LNi	−3.770	−1.760	2.01	3.77	1.76	2.77	−2.770	0.5	3.80
LCu	−6.680	−5.67	1.01	6.68	5.67	6.18	−6.180	0.99	37.94
ZnL	−8.170	−5.610	2.56	8.17	5.61	6.89	−6.890	0.39	18.51

Molecular docking studies

Perhaps the most important method for designing drug structures is molecular docking. By providing investigators gain insight into how the ligand and target receptor protein interact. This can help expedite and optimize the drug discovery process [14, 16, 17]. Furthermore, the approach we use predicts the conformation and binding affinities of various species to target proteins [16]. In this study, the interactions between the (LK) ligand and the active site *S. aureus* receptor (PDB ID: 2H92 and ID: 2CCJ) were investigated using molecular docking. Figure 6 and 7 show the information that has been obtained. The energy value of the related binding determined both the ligand's and the target protein's ability to dock towards that protein and the docking results. The more significant negative value of the binding energy represented these results. An evaluation of the binding scores obtained from the tested LK ligand's interaction with (ID: 2H92 and ID: 2CCJ). Figure 6 and 7 show the LK molecule attaching to (ID: 2H92, ID: 2CCJ) and adhering to the protein's hydrophobic surface. It was discovered that the LK molecule interacted most steadily with ARG 124, ARG 174, ARG 158, ARG 85, LYS 19, and ASP 154, ASP 31, GLY 123, shorter hydrogen bond, GLY 33 regions of protein ID: 2H92, while the LK molecule interacted most steadily with the shorter hydrogen bond TYR 99, TYR 96 and other interactions such as salt bridge, Pi-Cation, Pi-Anion, Pi-Pi, and attractive charge with amino acids like GLU 10, GLU 36, ARG 69, PHE 155, and PHE 65. The binding energy for these interactions with (ID: 2H92 and ID:2CCJ) was -8.80 kcal/mol and -9.00 kcal/mol, respectively.

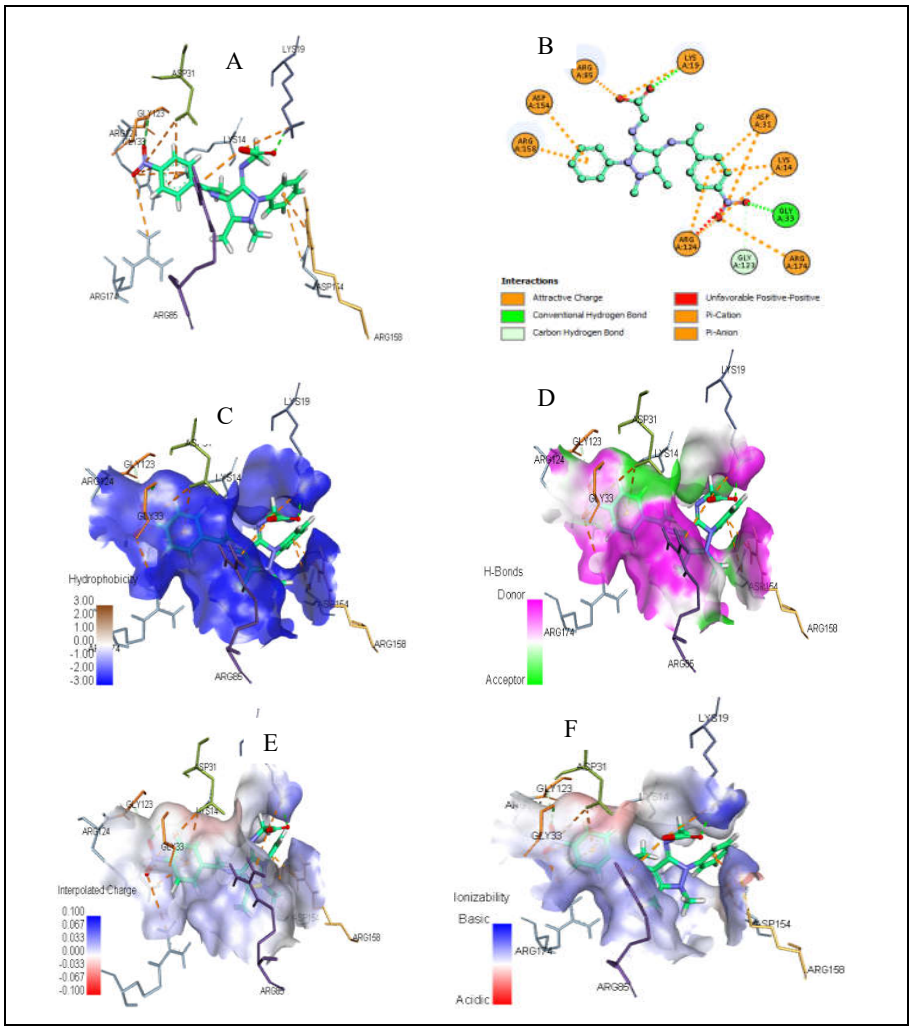

Figure 6. (A) 3D diagrams visualize interactions of (LK) with receptor ID: 2H92 of *S. aureus*, (B) 2D diagrams display interactions of (LK) with receptor ID: 2H92 of *S. aureus*, (C) display positions of hydrophobicity between enzyme and (LK) in ID: 2H92 of *S. aureus*, (D) represent positions of hydrogen bond between receptor ID: 2H92 of *S. aureus* and (LK), (E) show interpolated charge between ID: 2H92 of *S. aureus* and (LK), and (F) demonstrate ionizability regions for ID: 2H92 protein interaction around (LK).

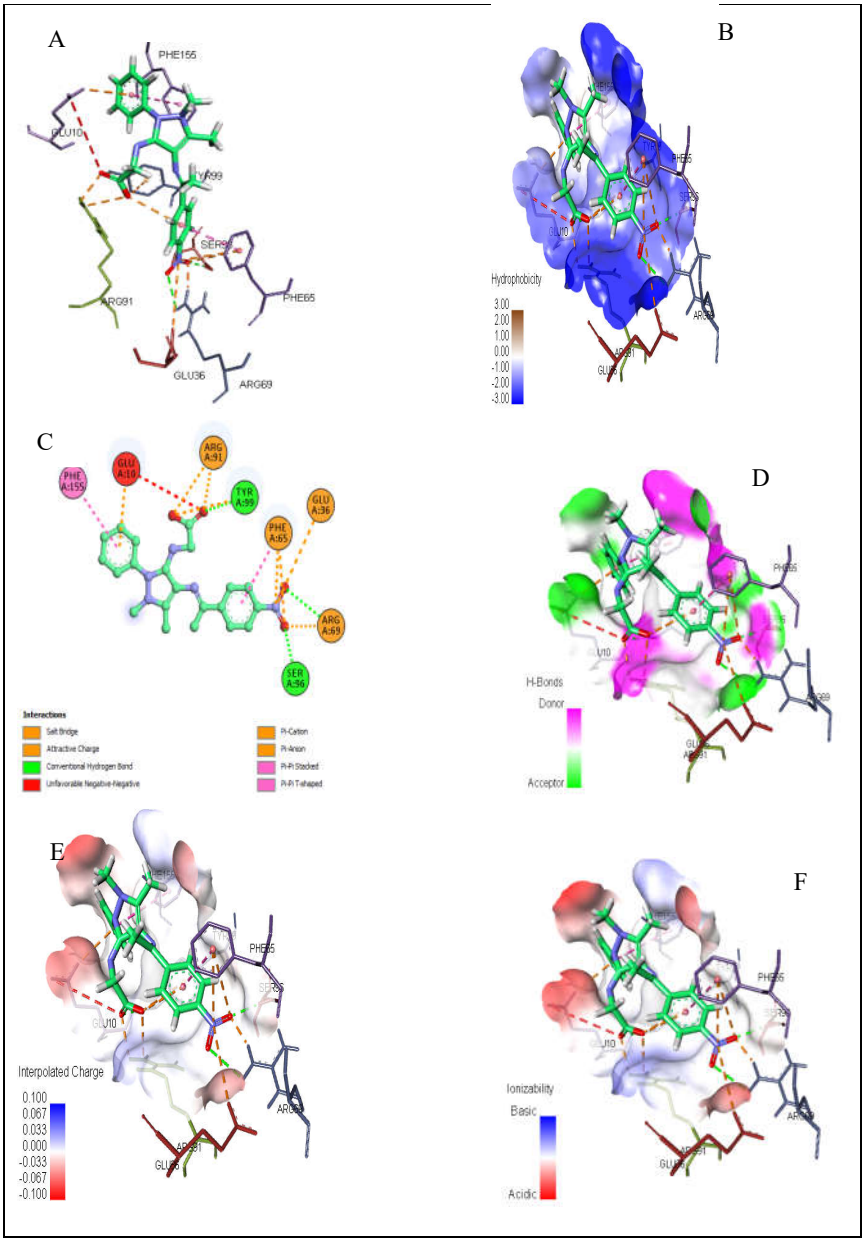

Figure 7. (A) 3D diagrams visualize interactions of (LK) with receptor ID: 2CCJ of *S. aureus*, (B) 2D diagrams display interactions of (LK) with receptor ID: 2CCJ of *S. aureus*, (C) display positions of hydrophobicity between enzyme and (LK) in ID: 2CCJ of *S. aureus*, (D) represent positions of hydrogen bond between receptor ID: 2CCJ of *S. aureus* and (LK), (E) show interpolated charge between ID: 2CCJ of *S. aureus* and (LK) and (F) demonstrate ionizability regions for ID: 2CCJ protein interaction around (LK).

Antibacterial activity

The chelating nature of the ligand, the variety of donor atoms, the complex's overall charge, a specific kind of metal ion. The chemical makeup of the opposing ions that balance the complex, and the geometrical structure of the complex are some of the elements that impact the biological properties of the complexes [18]. The antibacterial activity of Schiff base compounds may be greatly increased by including an imine group with chelating activities. These properties can be used to bind to bacterial cells at particular locations to inhibit their growth, while others can be utilized for moving metal across bacterial membranes. Additionally, the (KL) ligand, metal chelates exhibited antibacterial potential against *S. aureus*. Furthermore, the Cu(II) and Ni(II) complexes demonstrated higher antibacterial activity against *B. Subtilis* and *S. aureus*, while the Zn(II) complex showed the lowest antibacterial activity against *B. subtilis* and *S. aureus*. Moreover, LK exhibited the most promising antibacterial activity against both types of bacteria, Figure 8.

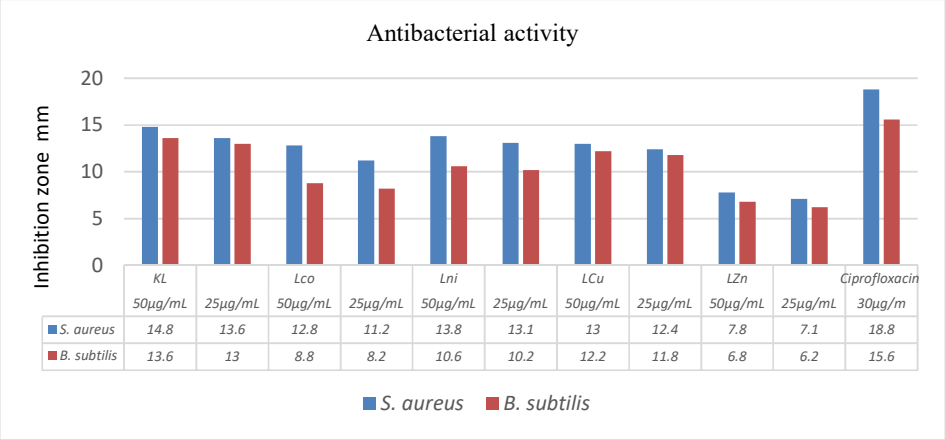

Figure 8. Inhibition zone of the synthesized compounds.

CONCLUSION

New potassium 2-(((E)-1,5-dimethyl-4-(((E)-1-(4-nitrophenyl)ethylidene)amino)-2-phenyl-1,2-dihydro-3H-pyrazol-3-ylidene)amino)acetate ligand-Co(II), Ni(II), Cu(II), and Zn(II) complexes were synthesized in this study. Spectroscopic and physicochemical methods were used to characterize their structures. According to the results, (LK) ligand acts as tri-dentate N and NO ligand and binds with the metal ion in a 1:1 molar ratio. The complexes adopted an octahedral geometry. Cu(II) and Zn(II) complexes' crystalline structures were examined using XRD data. The metal complexes' molecular structures were optimized theoretically and the DFT restrictions were computed. The antibacterial activity of the ligand and their corresponding complexes was examined in *vitro* against activity against *B. subtilis* and *S. aureus*. Additionally, molecular docking was applied to determine the examined ligand's ability to inhibit *S. aureus* (PDB ID: 2H92 and ID:2CCJ) demonstrated the strongest binding to the target receptor of this substance.

ACKNOWLEDGMENT

The authors are thankful to the University of Mosul, Department of Chemistry, College of Science, for their support and providing the research facilities to complete this work.

REFERENCES

1. Schiff, H. Mittheilungen aus dem Universitätslaboratorium in Pisa: Eine neueReihe organischer Basen. *J. Liebigs Ann. Chem.* **1864**, 131, 118-119.
2. Shaikh, S.; Dhavan, P.; Singh, P.; Uparkar, J.; Vaidya, S.P.; Jadhav, B.L.; Ramana, M.M.V. Design, synthesis and biological evaluation of novel antipyrine based α-amino phosphonates as anti-Alzheimer and anti-inflammatory agent. *J. Biomol. Struct. Dyn*. **2023**, 41, 386-401.
3. Mansor, M.; Ward, S.A.; Edwards, G. The effect of malaria infection on antipyrine metabolite formation in the rat. *J. Biol. Chem.* **1991**, 41,1264-1266.
4. Ali, S.M.; Azad, M.A.; Jesmin, M.; Ahsan, S.; Rahman, M.M.; Khanam, J.A.; Islam, M.N.; Shahriar, S.M. In vivo anticancer activity of vanillin semi carbazone. *Asian Pac. J. Trop. Biomed*. **2012**, 2, 438-442.
5. Raman, N.; Johnson, R.S.; Sakthivel, A. Transition metal complexes with Schiff-base ligands: 4-Aminoantipyrine based derivatives-a review. *J. Coord. Chem*. **2009**, 62, 691-709.
6. Raman, N.; Sakthivel, A.; Pravin, N. Exploring DNA binding and nucleolytic activity of few 4-aminoantipyrine based amino acid Schiff base complexes: A comparative approach. *Spectrochim. Acta Part A: Mol. Biomol. Spectrosc*. **2014**, 125, 404-413.
7. Raman, N.; Jeyamurugan, R.; Sudharsan, S.; Karuppasamy, K.; Mitu, L. Metal based pharmacologically active agents: Synthesis, structural elucidation, DNA interaction, in vitro antimicrobial and in vitro cytotoxic screening of copper(II) and zinc(II) complexes derived from amino acid based pyrazolone derivatives. *Arab. J. Chem.* **2013**, 6, 235-247.
8. Sakthivel, A.; Jeyasubramanian, K.; Thangagiri, B.; Raja, A.D. Recent advances in Schiff base metal complexes derived from 4-aminoantipyrine derivatives and their potential applications. *J. Mol. Struct.* **2020**, 1222, 128885.
9. Alwagaa, F.A.; Ahmed, S.A. Metal pharmacologically action agents: Mode of new tridentate glycine amino acid with diketone (benzil) and 4-aminoantipyrine complexes. *Egypt. J. Chem.* **2022**, 65, 59-67.
10. Abdou, A. Synthesis, structural, molecular docking, DFT, vibrational spectroscopy, HOMO-LUMO, MEP exploration, antibacterial and antifungal activity of new Fe(III), Co(II) and Ni(II) hetero-ligand complexes. *J. Mol. Struct.* **2022**, 1262. 132911.
11. Abu-Dief, A.M.; Alotaibi, N.H.; Al-Farraj, E.S.; Qasem, H.A.; Alzahrani, S.; Mahfouz, M.K.; Abdou, A. Fabrication, structural elucidation, theoretical, TD-DFT, vibrational calculation and molecular docking studies of some novel adenine imine chelates for biomedical applications. *J. Mol. Liq.* **2022**, 365, 119961.
12. Eltayeb, N.E.; Lasri, J.; Soliman, S.M.; Mavromatis, C.; Hajjar, D.; Elsilk, S.E.; Bandar A. Babgi, B.A.; Hussien, M.A. Crystal structure, DFT, antimicrobial, anticancer and molecular docking of (4E)-4-((aryl) methyleneamino)-1,2-dihydro-2,3-dimethyl-1-phenylpyrazol-5-one. *J. Mol. Struct.* **2020**, 1213, 128185.
13. Salem, M.A.; Ragab, A.; El-Khalafawy, A.; Makhlouf, A.H.; Askar, A.A.; Ammar, Y.A. Design, synthesis, in vitro antimicrobial evaluation and molecular docking studies of indol-2-one tagged with morpholinosulfonyl moiety as DNA gyrase inhibitors. *Bioorg. Chem.* **2020**, 96, 103619.
14. Ifeanyichukwu, I.; Eunice, E.U.; Ajoko, I.T.; Jim-Halliday, T.T. Molecular docking, synthesis and antimicrobial evaluation of 4-[(3-hydroxybenzalidene) amino] antipyrine and its copper complex. *Sch. Int. J. Chem. Mater. Sci*. **2023**, 6, 149-162.

15. Jones, R.C.; Malik, H.U. Analysis of minerals in oxide-rich soils by X-ray diffraction. *Quantitative Methods in Soil Mineralogy*, Soil Science Society of America, Inc.: USA; **1994**; pp. 296-329.
16. Thangarasu, S.; Chitradevi, A.; Siva, V.; Shameem, A.; Murugan, A.; Viswanathan, T.M.; Athimoolam, S.; Bahadur, S.A. Structural, spectroscopic, cytotoxicity and molecular docking studies of charge transfer salt: 4-Aminiumantipyrine salicylate. *Polycycl. Aromat. Comp.* **2023**, 43, 3159-3174.
17. Startseva, Y.D.; Hodyn, D.M.; Semenyuta, I.V. Undecylenic acid and N,N-dibutyl-undecenamide as effective antibacterials against antibiotic-resistant strains. *Ukr. Bio. Chem. J.* **2023**, 95, 55-63.
18. Vashistha, V.K.; Mittal, A.; Bala, R.; Dasa, D.K.; Singh, P.P. Synthesis, characterization, electrochemical and antibacterial studies of MN4-type macrocyclic complexes of Ni(II). *Rev. Roum. Chim* **2023**, 68, 447-452.